

## Characteristics of particulate matter collected at an urban background site and a roadside site in Birmingham, United Kingdom

Adewale M. TAIWO

*Division of Environmental Health Risk Management, School of Geography, Earth & Environmental Sciences, University of Birmingham, Edgbaston, Birmingham, B15 2TT, United Kingdom; currently at the Department of Environmental Management and Toxicology, Federal University of Agriculture, PMB 2240, Abeokuta, Ogun State, Nigeria.*  
Email: taiwoademat@gmail.com

Received: July 13, 2015; accepted: July 12, 2017

### RESUMEN

El objetivo del presente estudio fue investigar las características constitutivas del material particulado (MP) recolectado tanto en un contexto urbano (sitio de observación de Elms Road, SOER) como en un sitio ubicado junto al camino (sitio de observación de Bristol Road, SOBR). Las muestras de MP fueron recolectadas en los sitios receptores del 28 de marzo al 11 de abril de 2012. Los parámetros estudiados incluyeron iones solubles en agua ( $\text{Cl}^-$ ,  $\text{NO}_3^-$ ,  $\text{SO}_4^{2-}$ ,  $\text{Na}^+$ ,  $\text{NH}_4^+$ ,  $\text{K}^+$ ,  $\text{Mg}^{2+}$ ,  $\text{Ca}^{2+}$ ) y trazas de metales (V, Al, Cr, Mn, Fe, Zn, Cu, Sb, Ba, Pb). Los resultados mostraron mayores concentraciones de  $\text{NO}_3^-$ ,  $\text{NH}_4^+$ , Al y Fe en SOBR en comparación con SOER en relación con  $\text{MP}_{2.5}$ , y de  $\text{Cl}^-$ ,  $\text{NO}_3^-$ ,  $\text{Na}^+$ ,  $\text{K}^+$  y Fe con relación a  $\text{PM}_{2.5-10}$ , lo cual es indicativo de incrementos a lo largo del camino. Los componentes iónicos y metálicos de  $\text{MP}_{2.5}$  en SOER constituyeron 44 y 7% de la masa total de MP medida, respectivamente. Las proporciones de estas especies fueron 46 y 8% en SOBR. En cuanto al  $\text{MP}_{2.5-10}$ , los componentes solubles en agua y de trazas de metal representaron 42 y 12% en SOER, y 56 y 11% en SOBR.

### ABSTRACT

This study was conducted to investigate the compositional characteristics of particulate matter (PM) collected both at an urban background site (Elms Road observational site, EROS) and a roadside site (Bristol Road observational site, BROS). PM samples were collected at the receptor sites between March 28 and April 11, 2012. Observed parameters included water-soluble ions ( $\text{Cl}^-$ ,  $\text{NO}_3^-$ ,  $\text{SO}_4^{2-}$ ,  $\text{Na}^+$ ,  $\text{NH}_4^+$ ,  $\text{K}^+$ ,  $\text{Mg}^{2+}$ ,  $\text{Ca}^{2+}$ ) and trace metals (V, Al, Cr, Mn, Fe, Zn, Cu, Sb, Ba, Pb). Results showed higher concentrations of  $\text{NO}_3^-$ ,  $\text{NH}_4^+$ , Al and Fe at BROS than EROS regarding  $\text{PM}_{2.5}$ ; and  $\text{Cl}^-$ ,  $\text{NO}_3^-$ ,  $\text{Na}^+$ ,  $\text{K}^+$  and Fe regarding  $\text{PM}_{2.5-10}$ , indicating roadside increments. The ionic and metal components of  $\text{PM}_{2.5}$  at EROS constituted 44 and 7% of the total measured PM mass, respectively. The proportions of these species were 46 and 8% at BROS. For  $\text{PM}_{2.5-10}$ , water-soluble ions and trace metal components represented 42 and 12% at EROS, and 56 and 11% at BROS.

**Keywords:** Particulate matter, roadside increment, water-soluble ions, trace metals.

### 1. Introduction

Particles are emitted from numerous anthropogenic and natural activities. The prominent sources of particulate matter (PM) in cities and urban areas include: (a) traffic, (b) secondary, industrial, crustal, and marine combustion activities, and (c) power plants

(Levy et al., 2003; Charron and Harrison, 2005; Liu and Harrison, 2011; Taiwo et al., 2014). The presence of high concentrations of particulate matter could pose serious environmental and health concerns. Although measures have been put in place by developed nations to abate air pollution, epidemiological

studies still show that current air pollution episodes are capable of causing harm to the public. The Natural Resources Defense Council reported that particulate air pollution causes 64 000 deaths annually in the United States (Mysliwiec and Kleeman, 2002). In Europe, Watkiss et al. (2005) have reported around 350 000 annual premature deaths, while at the global scale more than one million deaths per year are recorded due to exposure to ambient particulate matter (WHO, 2009; Anenberg et al., 2010).

The contribution of traffic to  $PM_{2.5}$ ,  $PM_{2.5-10}$  and  $PM_{10}$  was researched by Liu and Harrison (2011) in the UK. The results showed a significant increment at roadside sites relative to urban background sites. This study also indicated industrial and marine aerosol as major contributors to coarse PM in the UK. A related study by Harrison et al. (2012) also showed an elevated mean concentration of  $PM_{2.5}$  at roadside sites as compared to background sites. The aim of this study is to compare PM compositional data collected at urban background and traffic sites.

## 2. Materials and methods

### 2.1 Description of the study areas

The Elms Road observatory site (EROS; 1.93° W, 52.46° N) is a typical urban background site, located on an open field within the University of Birmingham campus. The nearest roads are lightly trafficked and the nearby railway line carries mainly electric trains. The Bristol Road observatory site (BROS; 1.93° W, 52.45° N) is a traffic-polluted site also located within the University of Birmingham campus. These two sites are about 3.5 km southwest of the center of Birmingham, whose population is over one million and is part of a conurbation of 2.5 million people (Yin et al., 2010). EROS and BROS sites are shown in Figure 1.

### 2.2 Particulate matter sampling

Particle sampling was carried out with Partisol samplers placed at the two monitoring sites within the University of Birmingham for two weeks between March 28 and April 11.

### 2.3 Sample analysis

Prior to sampling and after this process, all filters were weighed with a Sartorius microbalance (Model MC 5; 1 pg sensitivity), which was equipped with a



Fig. 1. Location of EROS and BROS monitoring sites.

Polonium-210 anti-static source and had been subjected to at least 24 h pre-conditioning ( $25 \pm 5$  °C and  $30 \pm 10$  % RH) in our clean weighing room.

### 2.4 Metals analysis

All exposed Teflon filters were cut into two equal portions. One-half portion was digested for metal analysis by the reverse aqua regia procedures described in Harrison et al. (2003). Filters were digested in a solution of mixed concentrated acids (2.23 M HCl and 1.03 M  $HNO_3$ , ultra-pure grade) prepared by mixing concentrated nitric acid (65 ml) and concentrated hydrochloric acid (185 ml) in a 1000 cm volumetric flask and making up to 1 L with distilled deionized water. The mixed acid extractant (2 ml) was introduced into filters placed inside 4 ml narrow neck bottles and heated at 100 °C for 30 minutes in a water bath and then placed in an ultrasonic bath at 50 °C for another 30 min. This cycle was repeated and the ready digests transferred into 15 ml narrow neck bottles and made up to 10 ml with distilled deionized water. The ready extracts of filter samples were then analyzed using an inductively coupled plasma mass spectrometer (ICPMS, Agilent 7500 Ce) at the University of Birmingham. The version of this ICPMS is a quadrupole equipped with an octopole reaction system that removes interfering species. Metals of interest were Al, Mn, Cr, V, Fe, Zn, Cu, Ni, Cd, Sb, Ba and Pb. The mixed standards (from the stock 1000 mg  $L^{-1}$  VWR standard solution) were prepared in series of 0, 1, 5, 10, 20, 50 and 100  $\mu g L^{-1}$ . Internal standards used for ICPMS analysis were Sc, Ge, Y, In and Bi.

### 2.5 Water soluble ions analysis

The second half of the exposed filter samples was analyzed for water-soluble ions (cations  $\text{Na}^+$ ,  $\text{K}^+$ ,  $\text{Mg}^{2+}$ ,  $\text{Ca}^{2+}$ ,  $\text{NH}_4^+$ ; anions  $\text{Cl}^-$ ,  $\text{NO}_3^-$ ,  $\text{SO}_4^{2-}$ ,  $\text{C}_2\text{O}_4^{2-}$ ,  $\text{PO}_4^{3-}$ ). The filter samples were leached with 7.5 ml distilled deionized water in a Sonicator for 30 min. The leachates were measured with Dionex ICS 2000 and DX 500 for anions and cations, respectively.

An Ion Chromatography System (ICS) was employed for the analysis of water-soluble anions. The samples were loaded into an auto sampler in 0.5 ml vials. The sample was injected into the eluent stream of the instrument. For the anionic component (Dionex ICS 2000), the eluent used was potassium hydroxide (KOH). The eluent and the sample were pumped through an analytical (separator) column (AS 11 HC,  $2 \times 250$  mm) and a guard column (AG 11 HC,  $2 \times 50$  mm) for separation or ion exchange and contaminants removal, respectively (Thermo Fischer Scientific Inc., 2012). For water-soluble cations, the IC employed was Dionex DX 500 equipped with CS 12A analytical column ( $4 \times 250$  mm) and CG12A guard column ( $4 \times 50$  mm) (Thermo Fischer Scientific Inc., 2012). The eluent solution used was 1N methane sulphonic acid. Calibration curves (for anions and cations) were obtained with series of mixed standard solutions prepared in the range concentration between 0.5 and  $10 \text{ mg L}^{-1}$ . Ten blank filters were run for all the elemental concentrations to cancel the matrix effect of background levels.

## 3. Results

### 3.1 Partisol PM composition at EROS and BROS

Figures 2 and 3 show the mean mass and chemical composition of  $\text{PM}_{2.5}$  and  $\text{PM}_{2.5-10}$  at EROS and BROS. The two sites show higher mass concentration of  $\text{PM}_{2.5}$  than  $\text{PM}_{2.5-10}$ , signifying more influence of anthropogenic emissions. The two categories of PM were higher at BROS, probably due to traffic contribution. The water-soluble components of PM showed predominance of  $\text{NO}_3^-$  at BROS and  $\text{SO}_4^{2-}$  at EROS. The order of abundance of species in  $\text{PM}_{2.5}$  at EROS is as follows: sulphate (17% of  $\text{PM}_{2.5}$ ), nitrate (13%), ammonium (12%) and Al (6%). The water-soluble and trace metal species constituted 44 and 7% of the measured  $\text{PM}_{2.5}$  mass concentration, respectively. In the  $\text{PM}_{2.5-10}$  fraction, the sequence of abundance of species is as follows:  $\text{NO}_3^- > \text{Al} > \text{SO}_4^{2-} > \text{Cl}^- > \text{Ca}^{2+}$

$> \text{Na}^+/\text{Fe} > \text{Mg}^{2+}$ . These components represented 42 and 12%, respectively, for  $\text{PM}_{2.5-10}$ . The remaining components of PM could be attributable to carbonaceous species that were not measured during the study.

At BROS,  $\text{NO}_3^-$  constituted 20 and 24% of the total  $\text{PM}_{2.5}$  and  $\text{PM}_{2.5-10}$  mass concentration, respectively. The sequence followed 15 and 10% for  $\text{SO}_4^{2-}$ , 15 and 1% for  $\text{NH}_4^+$ , 1 and 7% for  $\text{Cl}^-$ , 1 and 4% for  $\text{Na}^+$ , 8 and 5% for Al, and 1 and 5% for Fe. Mg and  $\text{Ca}^{2+}$  occupied 1 and 4% of the  $\text{PM}_{2.5-10}$  mass, respectively. The measured components of  $\text{PM}_{2.5}$  showed dominance of water-soluble ions (46%), while trace metals only constituted 8%. A total fraction of 56% of the measured coarse mass concentration was attributed to ionic species and 11% to trace metals.

The influence of ammonium, nitrate and aluminium were prominent in  $\text{PM}_{2.5}$  at BROS while elevated  $\text{SO}_4^{2-}$ , V and Sb were observed at EROS. Cr, Mn, Zn and Cu exhibited similarities in their concentrations at the two sites. Higher values were clearly observed for coarse  $\text{Cl}^-$ ,  $\text{Na}^+$ ,  $\text{Mg}^{2+}$ ,  $\text{K}^+$ , Cr, Mn, Fe, Cu and Ba at BROS. Reasons might be linked to more pronounced traffic emissions from exhaust and non-exhaust vehicular processes, and additionally from the sea spray source for water-soluble species (Mazzei et al., 2008).

Figure 4 depicts the relationship between  $\text{PM}_{2.5}$  and  $\text{PM}_{2.5-10}$  mass concentrations measured at EROS and BROS sites.  $\text{PM}_{2.5}$  data at the two sites are well correlated with a slope near 1.0. The strong relationship between  $\text{PM}_{2.5}$  at the sites is a confirmation of a common emission source; however, the relationship between  $\text{PM}_{2.5-10}$  data at both sites was poorly defined. The contribution of coarse fraction to PM load was slightly higher at BROS than EROS. This might be directly linked to re-suspension of road dust at BROS. The  $\text{PM}_{2.5}/\text{PM}_{10}$  ratio has been calculated for Partisol samples at both sites, being 0.61 at EROS and 0.60 at BROS, which indicates anthropogenic emissions at these sites.

PM elemental differences between background (EROS) and roadside (BROS) sites are plotted in Fig. 5. There were convincing increments in the mean values of  $\text{NO}_3^-$ ,  $\text{NH}_4^+$ , Al and Fe at the roadside for  $\text{PM}_{2.5}$ ; and  $\text{Cl}^-$ ,  $\text{NO}_3^-$ ,  $\text{SO}_4^{2-}$ ,  $\text{Na}^+$ ,  $\text{K}^+$  and Fe for  $\text{PM}_{2.5-10}$ . Incremental parameters of Fe,  $\text{Cl}^-$ , and Al have been reported as markers for traffic in many published studies (Kleeman et al., 2000;

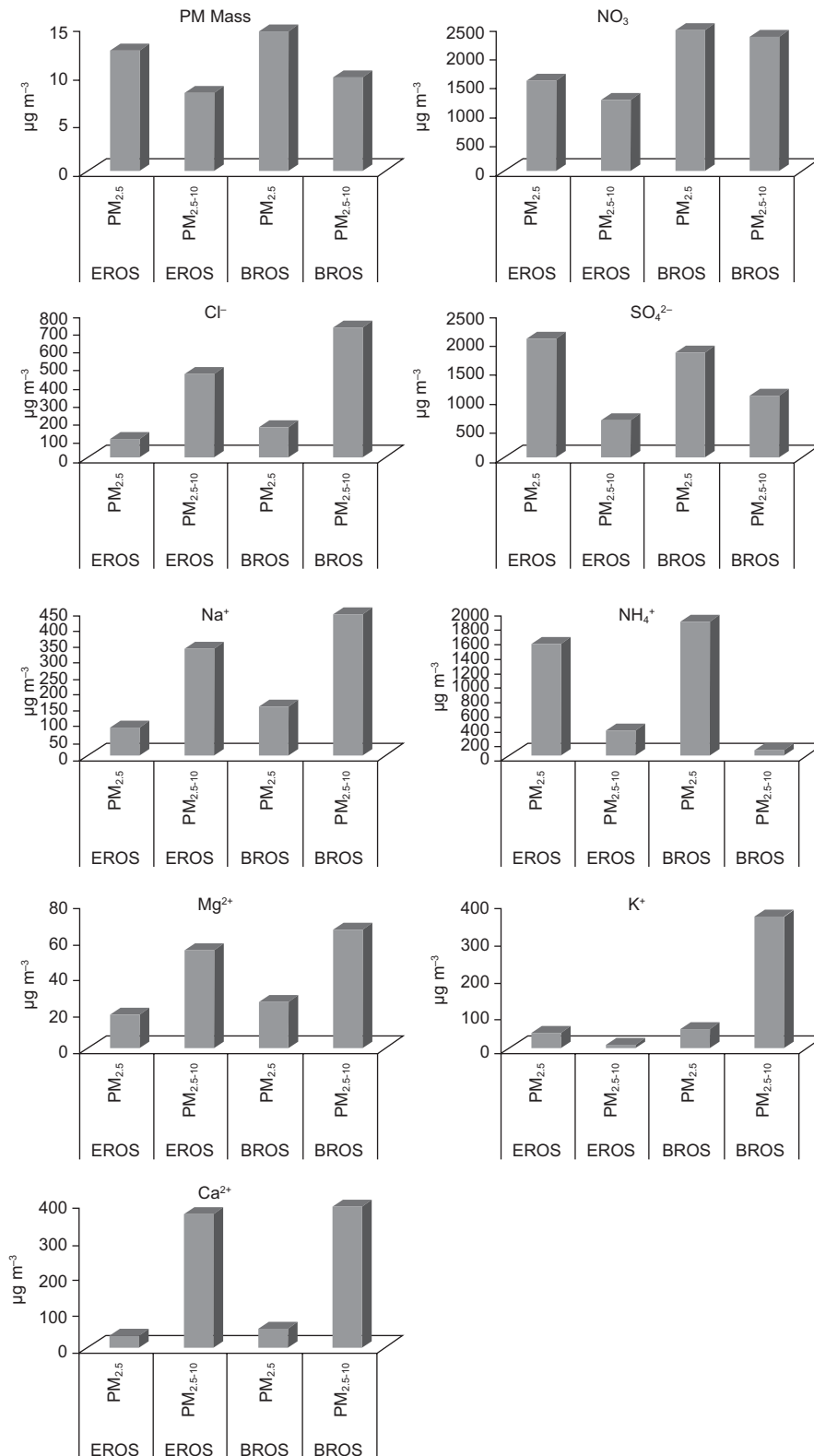


Fig. 2. Mass and water-soluble ions concentrations of PM analyzed in the study areas.

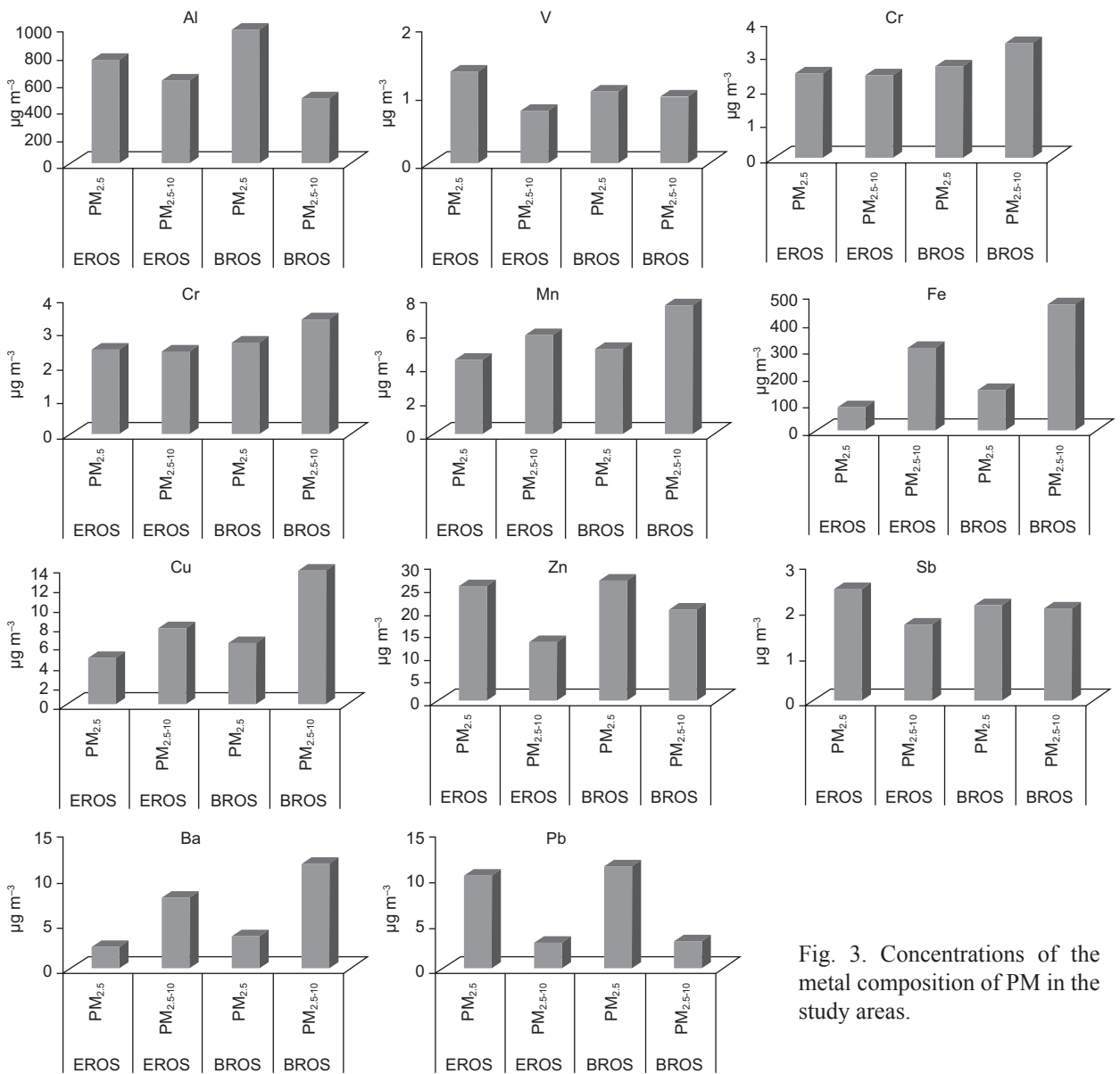


Fig. 3. Concentrations of the metal composition of PM in the study areas.

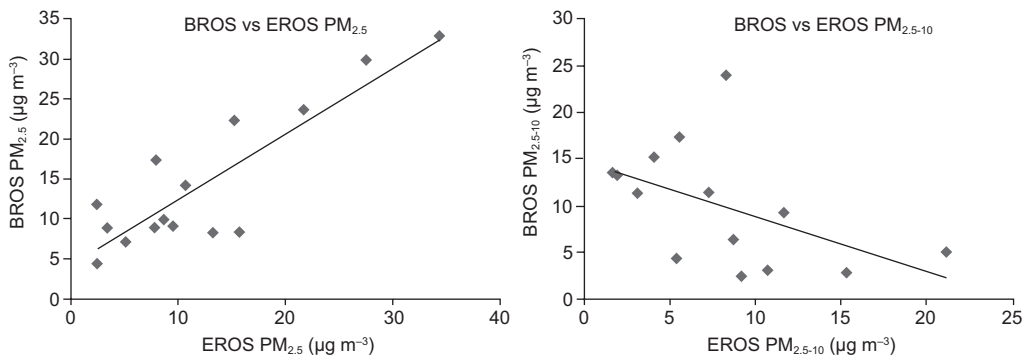


Fig. 4. Linear regression analysis of PM<sub>2.5</sub> and PM<sub>2.5-10</sub> at EROS and BROS.

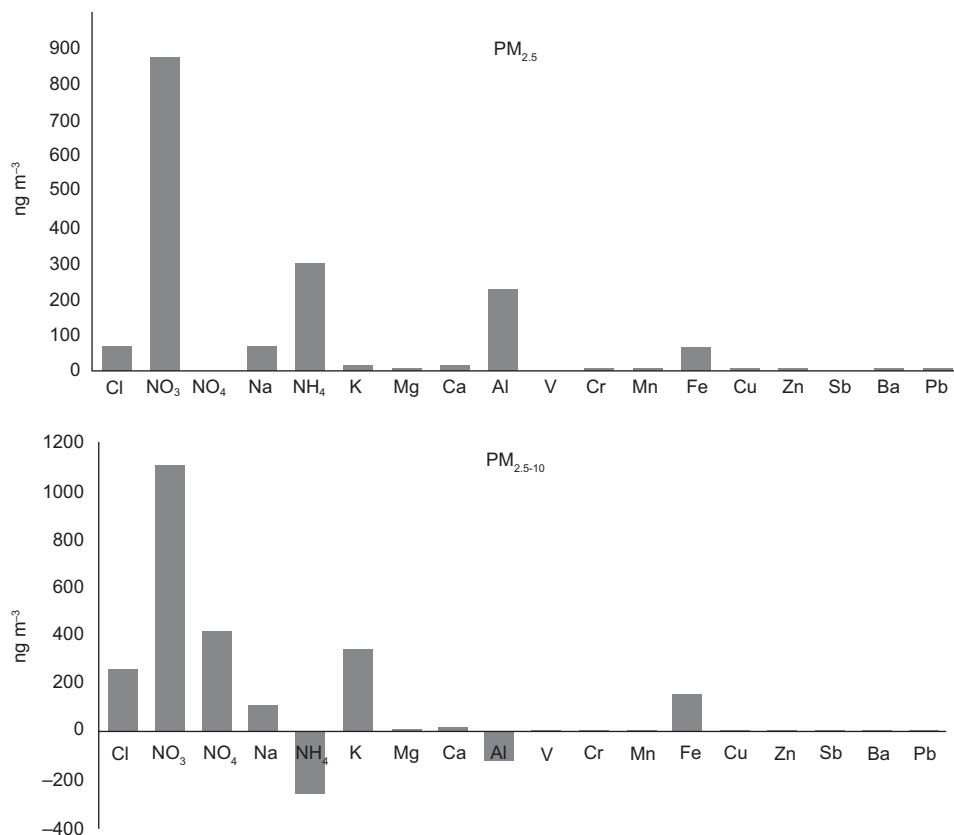


Fig. 5. PM elemental differences between background (EROS) and roadside (BROS) sites indicating roadside increments.

Chung et al., 2006; Lim et al., 2010; Xia and Gao, 2010). The higher values observed for roadside Na<sup>+</sup> and Cl<sup>-</sup> might be traced to de-icing of salt or marine aerosol (Harrison et al., 2004). The higher concentrations of roadside Fe observed for PM<sub>2.5</sub> and PM<sub>10</sub> were in good agreement with previous studies by Harrison et al. (2003).

### 3.2 Pearson's correlation coefficients for PM<sub>2.5</sub> and PM<sub>2.5-10</sub> data at EROS and BROS

Pearson's correlation coefficients ( $r$ ) of PM<sub>2.5</sub> and PM<sub>2.5-10</sub> at EROS and BROS are presented in Tables I-IV). EROS PM<sub>2.5</sub> mass concentration exhibited good agreement with NH<sub>4</sub><sup>+</sup>, K<sup>+</sup>, Fe, Cr, Mn, Cu, Zn, Sb, Ba and Pb ( $r = 0.56 - 0.86$ ;  $p < 0.05$  and  $0.01$ ). This shows that EROS fine PM might largely be influenced by woodsmoke/biomass burning, crustal sources and traffic emissions. A better correlation between K<sup>+</sup> and NH<sub>4</sub><sup>+</sup> ( $r = 0.74$ ;  $p < 0.01$ ) could indicate likely emissions from woodsmoke and incineration (Lim et al., 2010). Most of the trace metals were highly associated with one another, especially

Fe with Mn and Ba; and Sb with Ba, Zn, Fe and Pb. This could signify crustal and traffic emissions. The marine influence was prominent in EROS PM<sub>2.5</sub> with evidence of solid association between Na<sup>+</sup> and Cl<sup>-</sup> ( $r = 0.78$ ;  $p < 0.01$ ).

The PM<sub>2.5-10</sub> mass concentration at EROS showed strong correlations with NH<sub>4</sub><sup>+</sup>, K<sup>+</sup>, Ca<sup>2+</sup>, Fe, Cr, Mn, Cu, Zn, Ba and Pb ( $r = 0.68 - 0.86$ ;  $p < 0.01$ ). A strong relationship was established for Na<sup>-</sup> and Cl<sup>-</sup> ( $R = 0.95$ ;  $p < 0.01$ ). Mn and Fe were significantly correlated, indicating a similar emission source, probably crustal or industrial. Aluminum did not correlate well with Fe and Mn, suggesting their separate emission sources. Strong associations were established among the traffic signatures Sb, Fe, Cu, Zn and Ba in coarse PM.

Pearson's correlations for PM<sub>2.5</sub> mass with other constituents at BROS were similar to those observed at EROS. The association of NH<sub>4</sub><sup>+</sup> with SO<sub>4</sub> and NO<sub>3</sub>, though weak, were better defined in PM<sub>2.5</sub> at BROS than at EROS. Mg and Ca were also strongly

Table I. Pearson's correlation coefficients of Partisol PM<sub>2.5</sub> chemical species at EROS.

	Mass	Cl	NO <sub>3</sub>	SO <sub>4</sub>	Na	NH <sub>4</sub>	K	Mg	Ca	Al	Fe	V	Cr	Mn	Cu	Zn	Sb	Ba	Pb
Mass	1	0.216	0.075	-0.213	-0.191	0.864**	0.860**	-0.351	0.079	-0.209	0.778**	0.342	0.565*	0.683**	0.558*	0.734**	0.786**	0.668*	0.836**
Cl		1	0.029	-0.255	0.775**	0.552	0.354	0.590	0.245	-0.162	0.586*	0.663*	0.360	0.363	-0.258	0.326	-0.303	-0.020	0.270
NO <sub>3</sub>			1	0.622*	-0.047	-0.056	0.258	0.463	-0.024	0.099	0.467	0.302	-0.139	0.361	0.107	0.289	0.296	0.591*	0.163
SO <sub>4</sub>				1	-0.191	-0.303	0.161	0.161	0.054	0.787**	0.177	0.187	-0.329	0.194	-0.034	0.071	0.075	0.400	-0.179
Na					1	0.069	-0.006	0.972**	0.083	-0.207	0.037	0.356	0.018	0.025	-0.428	-0.087	-0.479	-0.293	-0.007
NH <sub>4</sub>						1	0.745**	-0.207	0.193	-0.265	0.724**	0.602*	0.839**	0.682**	0.265	0.769**	0.426	0.388	0.806**
K							1	-0.064	0.146	0.250	0.791**	0.703*	0.744**	0.877**	0.837**	0.866**	0.683*	0.720*	0.857**
Mg								1	0.219	-0.100	-0.014	0.139	-0.213	0.006	-0.336	-0.324	-0.486	-0.087	-0.167
Ca									1	0.270	0.147	0.165	0.177	0.569*	0.173	0.060	0.344	0.417	0.017
Al										1	-0.123	0.111	-0.260	0.091	-0.072	-0.085	-0.037	0.155	-0.273
Fe											1	0.643**	0.534*	0.787**	0.412	0.860**	0.670*	0.738**	0.761**
V												1	0.710*	0.564*	0.235	0.755**	0.058	0.281	0.630*
Cr													1	0.608*	0.752**	0.808**	0.268	0.252	0.802**
Mn														1	0.456	0.790**	0.795**	0.888**	0.748**
Cu															1	0.530*	0.778**	0.774**	0.861**
Zn																1	0.598*	0.644*	0.910**
Sb																	1	0.895**	0.617*
Ba																		1	0.603*
Pb																			1

\* p < 0.05; \*\* p < 0.01.

Table II. Pearson's correlation coefficients of Partisol PM<sub>2.5-10</sub> chemical species at EROS.

	Mass	Cl	NO <sub>3</sub>	SO <sub>4</sub>	Na	NH <sub>4</sub>	K	Mg	Ca	Al	Fe	V	Cr	Mn	Cu	Zn	Sb	Ba	Pb
Mass	1	0.246	-0.378	-0.373**	0.062	0.785**	0.726**	0.154	0.684**	0.060	0.878**	0.259	0.797**	0.847**	0.665**	0.837**	0.624	0.729**	0.864**
Cl		1	-0.327	-0.518	0.946**	-0.020	0.599*	0.909**	-0.085	0.308	0.059	-0.276	0.077	-0.075	-0.216	-0.160	-0.415	-0.246	0.039
NO <sub>3</sub>			1	0.721**	-0.229	-0.088	-0.147	-0.219	-0.365	-0.222	-0.529	-0.074	-0.513	-0.364	-0.238	-0.313	0.679*	-0.292	-0.528
SO <sub>4</sub>				1	0.002	-0.294	-0.365*	-0.350	-0.194	-0.105	-0.023*	-0.369	0.196	-0.328	-0.181*	-0.235	0.187*	-0.186*	-0.426
Na					1	-0.207	0.581*	0.981**	-0.233	0.388	-0.124	-0.273	-0.066	-0.265	-0.409	-0.183	-0.462	-0.326	-0.009
NH <sub>4</sub>						1	0.648*	-0.186	0.399	-0.141	0.578	0.317	0.343	0.703*	0.836**	0.586	0.872**	0.812**	0.550
K							1	0.619*	0.157	0.140	0.424	0.037	0.372	0.364	0.202	0.455	0.313	0.356	0.594*
Mg								1	-0.082	0.408	-0.009	-0.211	0.070	-0.136	-0.314	-0.065	-0.349	-0.212	0.106
Ca									1	-0.059	0.874**	0.324	0.890**	0.932*	0.842**	0.820*	0.735*	0.856**	0.736**
Al										1	-0.099	0.511	-0.012	-0.037	-0.119	-0.175	-0.276	-0.157	0.022
Fe											1	0.189	0.922**	0.926**	0.763**	0.930**	0.687*	0.827**	0.886**
V												1	0.245	0.454	0.566*	0.199	0.544	0.519	0.383
Cr													1	0.891**	0.690**	0.884**	0.561	0.747**	0.936**
Mn														1	0.926**	0.909**	0.896**	0.951**	0.871**
Cu															1	0.748*	0.985**	0.988**	0.694*
Zn																1	0.672*	0.815**	0.905**
Sb																	1	0.983**	0.617
Ba																		1	0.770**
Pb																			1

\* p &lt; 0.05; \*\* p &lt; 0.01.

Table III. Pearson's correlation coefficients of Partisol PM<sub>2.5</sub> chemical species at BROS.

	Mass	Cl	NO <sub>3</sub>	SO <sub>4</sub>	Na	NH <sub>4</sub>	K	Mg	Ca	Al	Fe	V	Cr	Mn	Cu	Zn	Sb	Ba	Pb
Mass	1	0.006	0.222	0.485	-0.015	0.891**	0.791**	-0.068	0.039	-0.292	0.900**	0.085	0.558*	0.476	0.495	0.754**	0.562*	0.466	0.760**
Cl		1	-0.195	-0.046	0.290	-0.001	-0.186	0.204	0.370	-0.117	0.052	-0.373	0.106	-0.200	-0.288	-0.086	-0.313	-0.335	-0.159
NO <sub>3</sub>			1	0.709**	-0.211	0.198	0.378	-0.111	-0.252	0.373	0.095	-0.332	-0.200	0.038	0.024	-0.084	0.100	0.158	0.073
SO <sub>4</sub>				1	-0.322	0.355	0.761**	-0.276	-0.208	-0.130	0.441	-0.213	-0.061	0.398	0.334	0.196	0.382	0.470	0.372
Na					1	-0.239	-0.258	0.988**	0.443	0.238	-0.143	0.009	-0.240	-0.267	-0.390	-0.253	-0.260	-0.245	-0.244
NH <sub>4</sub>						1	0.686**	-0.302	-0.003	-0.351	0.802**	0.025	0.658*	0.402	0.448	0.643**	0.478	0.330	0.583*
K							1	-0.337	-0.264	-0.384	0.696**	-0.035	0.308	0.610*	0.586*	0.519	0.610*	0.668**	0.641*
Mg								1	0.704*	0.522	-0.076	0.234	-0.266	-0.054	-0.354	-0.240	-0.123	-0.014	-0.250
Ca									1	-0.014	0.313	0.324	0.270	0.276	0.152	0.220	0.184	0.149	0.111
Al										1	-0.392	-0.104	-0.375	-0.380	-0.407	-0.405	-0.314	-0.377	-0.397
Fe											1	0.204	0.665**	0.637*	0.632*	0.855**	0.659**	0.573*	0.809**
V												1	0.207	0.389	0.451	0.380	0.425	0.354	0.280
Cr													1	0.512	0.641**	0.804**	0.636*	0.345	0.594*
Mn														1	0.957**	0.673**	0.935**	0.953**	0.725**
Cu															1	0.778**	0.975**	0.911**	0.786**
Zn																1	0.794**	0.622*	0.933**
Sb																	1	0.900**	0.814**
Ba																		1	0.756**
Pb																			1

\* p < 0.05; \*\* p < 0.01.

Table IV. Pearson's correlation coefficients of Partisol PM<sub>2.5-10</sub> chemical species at BROS.

	Mass	Cl	NO <sub>3</sub>	SO <sub>4</sub>	Na	NH <sub>4</sub>	K	Mg	Ca	Al	Fe	V	Cr	Mn	Cu	Zn	Sb	Ba	Pb
Mass	1	-0.459	0.365	0.286	-0.083	-0.287	-0.121	-0.184	-0.591*	0.000	-0.478	-0.202	-0.481	-0.454	-0.447	-0.397	-0.422	-0.492	-0.429
Cl		1	-0.364	-0.331	0.281	0.202	0.273	0.287	-0.127	0.186	0.017	-0.200	-0.116	-0.376	-0.446	0.234	-0.471	-0.411	-0.175
NO <sub>3</sub>			1	0.889**	-0.056	-0.354	-0.035	-0.076	-0.526*	-0.138	-0.430	-0.292	-0.347	-0.226	-0.159	-0.413	-0.163	-0.198	-0.305
SO <sub>4</sub>				1	-0.151	-0.059	-0.053	-0.058	-0.442	-0.322	-0.305	-0.236	-0.145	-0.041	-0.017	-0.267	-0.009	-0.028	-0.150
Na					1	0.451	0.989**	0.979**	-0.236	0.440	-0.224	-0.554*	-0.206	-0.318	-0.267	0.199	-0.281	-0.231	-0.261
NH <sub>4</sub>						1	0.373	0.444	0.021	0.168	-0.107	-0.107	-0.133	0.005	0.156	-0.055	0.086	0.078	-0.064
K							1	0.975**	-0.267	0.424	-0.293	-0.505	-0.232	-0.309	-0.237	0.193	-0.255	-0.203	-0.256
Mg								1	-0.085	0.478	-0.075	-0.492	-0.049	-0.189	-0.175	0.268	-0.188	-0.127	-0.126
Ca									1	0.039	0.862**	0.519*	0.887**	0.855**	0.737**	0.485	0.752**	0.800**	0.786**
Al										1	-0.181	-0.219	-0.183	-0.206	-0.179	-0.163	-0.190	-0.211	-0.180
Fe											1	0.411	0.949**	0.752**	0.523*	0.626*	0.542*	0.638*	0.771**
V												1	0.423	0.580*	0.584*	0.431	0.562*	0.559*	0.766**
Cr													1	0.849**	0.647**	0.601*	0.673**	0.760**	0.805**
Mn														1	0.942**	0.481	0.952**	0.972**	0.814**
Cu															1	0.402	0.997**	0.982**	0.694**
Zn																1	0.392	0.484	0.601*
Sb																	1	0.986**	0.694**
Ba																		1	0.750**
Pb																			1

\* p &lt; 0.05; \*\* p &lt; 0.01.

correlated. Traffic signatures of Sb, Fe, Cu, Zn and Ba exhibited stronger correlations at BROS.

The sea salt aerosols ( $\text{Na}^+$ ,  $\text{Cl}^-$ ) are weakly correlated at BROS. In the  $\text{PM}_{2.5-10}$  fraction at BROS, mass concentration shows negative correlation with most observed constituents.  $\text{Na}^+$ ,  $\text{K}^+$  and  $\text{Mg}^{2+}$  are strongly associated (0.98 – 0.99;  $p < 0.01$ ) in the coarse PM component at BROS, confirming probable influence from the road re-suspension dust. The traffic elements were also strongly associated at BROS for  $\text{PM}_{2.5-10}$  as observed in EROS.

Table V shows the inter-site relationship among the measured components of  $\text{PM}_{2.5}$  and  $\text{PM}_{2.5-10}$  at EROS and BROS. These sites are about 250 m apart; hence, they could be influenced by a related factor, being traffic the major suspect. Strong relationships

Table V. Inter-site correlations between PM in EROS and BROS.

Components	Coefficient ( $R^2$ )	Components	Coefficient ( $R^2$ )
$\text{PM}_{2.5}$ mass	0.87**	Al	0.20
$\text{Cl}^-$	0.55	V	0.92**
$\text{NO}_3^-$	0.12	Cr	-0.17
$\text{SO}_4^{2-}$	0.36	Mn	0.87**
$\text{Na}^+$	0.29	Fe	0.81**
$\text{NH}_4^+$	0.86**	Cu	0.54*
$\text{K}^+$	0.62*	Zn	0.92**
$\text{Mg}^{2+}$	0.68*	Sb	0.85**
$\text{Ca}^{2+}$	0.44	Ba	0.89**
		Pb	0.71**
$\text{PM}_{2.5-10}$ mass	-0.33	Al	-0.10
$\text{Cl}^-$	0.73**	V	0.87**
$\text{NO}_3^-$	0.18	Cr	0.07
$\text{SO}_4^{2-}$	-0.01	Mn	0.84**
$\text{Na}^+$	0.22	Fe	0.86**
$\text{NH}_4^+$	0.30	Cu	0.88*
$\text{K}^+$	-0.20	Zn	0.48
$\text{Mg}^{2+}$	0.05	Sb	0.91**
$\text{Ca}^{2+}$	0.90**	Ba	0.91**
		Pb	0.61*

\*  $p < 0.05$ ; \*\*  $p < 0.01$ .

were also observed at EROS and BROS for  $\text{PM}_{2.5}$  and  $\text{PM}_{2.5-10}$  components of V, Mn, Fe, Cu, Zn, Sb, Ba and Pb. Species such as  $\text{NH}_4^+$ ,  $\text{K}^+$ ,  $\text{Mg}^{2+}$  and Zn showed better associations at EROS and BROS for fine PM; while  $\text{Cl}^-$  and  $\text{Ca}^{2+}$  were better correlated in the coarse PM at the two sites.

#### 4. Discussion

Most of the PM components (including mass concentrations) measured at the EROS background site were generally lower than those at BROS, a typical traffic-polluted site. This is not surprising due to the roadside increment of pollutants. Elemental difference between fine  $\text{SO}_4^{2-}$  and coarse  $\text{NH}_4^+$  at EROS and BROS were 245 and 262  $\text{ng m}^{-3}$ . Conversely, higher concentrations of coarse  $\text{SO}_4^{2-}$  and fine  $\text{NH}_4^+$  were measured at BROS with an incremental difference of 415 and 298  $\text{ng m}^{-3}$ , respectively. Since the two sites were within the University of Birmingham, insignificant regional transportation of these pollutants is expected (Harrison et al., 2004). The discrepancies in  $\text{NH}_4^+$  measured at the two sites might be related to emission sources like biomass burning or incineration (Lim et al., 2010). Elevated coarse  $\text{SO}_4^{2-}$  at BROS may be attributable to road resuspended dust or soil (Harrison et al., 1997). A large difference was found in nitrate concentrations between the two sites for fine (875  $\text{ng m}^{-3}$ ) and coarse (1108  $\text{ng m}^{-3}$ ) PM, which is an evidence of a distinctive roadside emission. Higher  $\text{PM}_{2.5}$  and  $\text{PM}_{2.5-10}$  mass concentrations at BROS also indicate traffic contributions from vehicular emissions and road re-suspension. Harrison et al. (1997) found a very strong correlation between  $\text{PM}_{2.5}$  and  $\text{NO}_x$ , suggesting that the  $\text{PM}_{2.5}$  mass concentration could be adopted as a better traffic signature.

This study showed elevated  $\text{SO}_4^{2-}$ , lower  $\text{NO}_3^-$  and  $\text{Cl}^-$  values in the  $\text{PM}_{2.5}$  component relative to the research recently published by Laongsri and Harrison (2013) at EROS. In the  $\text{PM}_{2.5-10}$  component,  $\text{NO}_3^-$  and  $\text{SO}_4^{2-}$  concentrations in this study are about two times higher than concentrations reported by Laongsri and Harrison (2013), but  $\text{Cl}^-$  concentrations are lower. At BROS, a previous study of Yin et al. (2010) for  $\text{Cl}^-$ ,  $\text{SO}_4^{2-}$ ,  $\text{NO}_3^-$ , Ca and Fe in  $\text{PM}_{10}$  found that these components represent approximately 3, 9, 6, 1 and 4% of the total measured mass, respectively. In this study, the corresponding values of these components

in  $PM_{10}$  (computed by addition of  $PM_{2.5}$  and  $PM_{2.5-10}$ ) were 4, 12, 20, 2 and 5%, respectively. Except for  $NO_3^-$ , where a relatively higher fraction was measured, it appeared that the other observed components are in good agreement with Yin et al. (2010). The wide difference observed in the percentages of these secondary aerosols (nitrate and sulphate) relative to previously reported values at these sites might still be linked with regional influence rather than local emissions (Abdalmogith et al., 2006). Other probable reasons for this lack of agreement may be attributable to different sampling times and meteorological conditions.

Aluminum showed an increment for fine PM at BROS while the opposite occurred for coarse PM, which exhibited higher amounts at EROS. Fine Al can be attributed to vehicular emissions while coarse Al may take its source from soil. Traffic signatures such as Zn, Fe, Cu, Ba, Mn and Pb (Thorpe and Harrison, 2008) showed greater concentrations in fine and coarse PM at BROS, which agrees with studies conducted at roadsides (Amato et al., 2009, 2011; Gietl et al., 2010). Pearson correlation coefficients depicted in Table I revealed strong significant correlations among these traffic signatures for  $PM_{2.5-10}$  showing the pronounced contribution by traffic at both sites.

The  $PM_{2.5}/PM_{10}$  ratios observed at EROS and BROS showed dominance of anthropogenic emissions at the two sites. This is comparable to most studies reported at urban sites. The earlier study of Yin and Harrison (2008) has observed  $PM_{2.5}/PM_{10}$  ratio of 0.60 at BROS in perfect agreement with this present study. In the Harrison et al. (2004) study at an urban background site in London (High Holborn), the ratio of  $PM_{2.5}/PM_{10}$  was calculated as 0.62 while the value was 0.64 at the roadsides. Across the UK, the mean ratio of  $PM_{2.5-10}/PM_{10}$  has been reported as  $0.31 \pm 0.13$  (Liu and Harrison, 2011). This indicates dominance of  $PM_{2.5}$  in agreement with observations at BROS and EROS.

## 5. Conclusions

The above-mentioned data of EROS and BROS depicts higher concentrations of most PM parameters at the BROS site, which reflects the roadside increment. Sulphate was the most preponderant fine particle at EROS (17% of the  $PM_{2.5}$  mass), while nitrate was

predominant at BROS (20%). In the coarse fraction, nitrate was the highest chemical component at both sites (15 and 24% at EROS and BROS, respectively). The measured chemical components of PM (ionic and metal species) constituted only 51 and 54% of  $PM_{2.5}$ , and 54% and 67% of  $PM_{2.5-10}$  at EROS and BROS, respectively. The remaining components can be attributed to the unmeasured carbonaceous species, mass-associated oxygen, particle-bound water and other chemical constituents.

## Acknowledgments

The author is grateful to the Tertiary Education Trust Fund of the Federal University of Agriculture, Abeokuta, Nigeria for sponsoring my research work at the University of Birmingham, UK.

## References

- Abdalmogith S.A., R.M. Harrison and R.G. Derwen, 2006. Particulate sulphate and nitrate in Southern England and Northern Ireland during 2002/3 and its formation in a photochemical trajectory model. *Sci. Tot. Environ.* 368, 769-780. doi: 10.1016/j.scitotenv.2006.02.047
- Amato F., M. Pandolfi, A. Escrig, X. Querol, A. Alastuey, J. Pey, N. Prez and P.K. Hopke, 2009. Quantifying road dust resuspension in urban environment by Multilinear Engine: A comparison with PMF2. *Atmos. Environ.* 43, 2770-2780. doi: 10.1016/j.atmosenv.2009.02.039
- Anenberg S.C., L.W. Horowitz, D.Q. Tong and J.J. West, 2010. An estimate of the global burden of anthropogenic ozone and fine particulate matter on premature human mortality using atmospheric modeling. *Environ. Health Perspect.* 118, 1189-1195. doi: 10.1289/ehp.0901220
- Charron A. and R.M. Harrison, 2005. Fine ( $PM_{2.5}$ ) and coarse ( $PM_{2.5-10}$ ) particulate matter on a heavily trafficked London highway: Sources and processes. *Environ. Sci. Technol.* 39, 7768-7776. doi: 10.1021/es050462i
- Chung Y.-S., S.-H. Kim, J.-H. Moon, Y.-J. Kim, J.-M. Lim and J.-H. Lee, 2006. Source identification and long-term monitoring of airborne particulate matter ( $PM_{2.5}/PM_{10}$ ) in an urban region of Korea. *J. Radioanal. Nucl. Chem.* 267, 35-48. doi: 10.1007/s10967-006-0006-z
- Gietl J.K., R. Lawrence, A.J. Thorpe and R.M. Harrison, 2010. Identification of brake wear particles and derivation of a quantitative tracer for brake dust at a major

- road. *Atmos. Environ.* 44, 141-146.  
doi: 10.1016/j.atmosenv.2009.10.016
- Harrison R.M., A.R. Deacon and M.R. Jones, 1997. Sources and processes affecting concentrations of PM<sub>10</sub> and PM<sub>2.5</sub> particulate matter in Birmingham (U.K.). *Atmos. Environ.* 31, 4103-4117.  
doi: 10.1016/S1352-2310(97)00296-3
- Harrison R.M., A.M. Jones and R.G. Lawrence, 2003. A pragmatic mass closure model for airborne particulate matter at urban background and roadside sites. *Atmos. Environ.* 37, 4927-4933.  
doi: 10.1016/j.atmosenv.2003.08.025
- Harrison R.M., A.M. Jones and R.G. Lawrence, 2004. Major component composition of PM<sub>10</sub> and PM<sub>2.5</sub> from roadside and urban background sites. *Atmos. Environ.* 38, 4531-4538. doi: /10.1016/j.atmosenv.2004.05.022
- Harrison R.M., D. Laxen, S. Moorcroft and K. Laxen, 2012. Processes affecting concentrations of fine particulate matter (PM<sub>2.5</sub>) in the UK atmosphere. *Atmos. Environ.* 46, 115-124. doi: 10.1016/j.atmosenv.2004.05.022
- Kleeman M.J., J.J. Schauer and G.R. Cass, 2000. Size and composition distribution of fine particulate matter emitted from motor vehicles. *Environ. Sci. Technol.* 34, 1132-1142. doi: 10.1021/es981276y
- Laongsri B. and R.M. Harrison, 2013. Atmospheric behaviour of particulate oxalate at UK urban background and rural sites. *Atmos. Environ.* 71, 319-326.  
doi: 10.1016/j.atmosenv.2013.02.015
- Levy J.I., D.H. Bennett, S.J. Melly and J.D. Spengler, 2003. Influence of traffic patterns on particulate matter and polycyclic aromatic hydrocarbon concentrations in Roxbury, Massachusetts. *J. Expo. Anal. Environ. Epidemiol.* 13, 364-71. doi: 10.1038/sj.jea.7500289
- Lim J.-M., J.-H. Lee, J.-H. Moon, Y.-S. Chung and K.-H. Kim, 2010. Source apportionment of PM<sub>10</sub> at a small industrial area using positive matrix factorization. *Atmos. Res.* 95, 88-100.  
doi: 10.1016/j.atmosres.2009.08.009
- Liu J.-Y. and R.M. Harrison, 2011. Properties of coarse particles in the atmosphere of the United Kingdom. *Atmos. Environ.* 45, 3267-3276.  
doi: 10.1016/j.atmosenv.2011.03.039
- Mazzei F., A. D'Alessandro, F. Lucarelli, S. Nava, P. Prati, G. Valli and R. Vecchi, 2008. Characterization of particulate matter sources in an urban environment. *Sci. Tot. Environ.* 401, 81-89.  
doi: 10.1016/j.scitotenv.2008.03.008
- Mysliwiec M.J. and M.J. Kleeman, 2002. Source apportionment of secondary airborne particulate matter in a polluted atmosphere. *Environ. Sci. Technol.* 36, 5376-5384. doi: 10.1021/es020832s
- Taiwo A.M., D.C.S. Beddows, Z. Shi and R.M. Harrison, 2014. Mass and number size distributions of particulate matter components: Comparison of an industrial site and an urban background site. *Sci. Tot. Environ.* 475, 29-38.  
doi: 10.1016/j.scitotenv.2013.12.076
- Thermo Fischer Scientific Inc., 2012. Dionex ICS-2100 Ion Chromatography System Operator's Manual. Document No. 065291. Available at: <http://www.dionex.com/en-us/webdocs/73382-Man-IC-IC-S2100-Operators-Oct2012-DOC065291-03.pdf> (last accessed on August 8, 2013).
- Thorpe A. and R.M. Harrison, 2008. Sources and properties of non-exhaust particulate matter from road traffic: a review. *Sci. Tot. Environ.* 400, 270-282.  
doi: 10.1016/j.scitotenv.2008.06.007
- Watkiss P., S. Pye and M. Holland, 2005. Baseline scenarios for service contract for carrying out cost-benefit analysis of air quality related issues, in particular in the Clean Air for Europe (CAFE) programme. AEAT/ED51014/ Baseline Issue 5. Didcot, United Kingdom.
- WHO, 2009. Global health risks: Mortality and burden of disease attributable to selected major risks. World Health Organization, Geneva. Available at: [http://whqlibdoc.who.int/publications/2009/9789241563871\\_eng.pdf](http://whqlibdoc.who.int/publications/2009/9789241563871_eng.pdf) (last accessed on July 17, 2013).
- Xia L. and Y. Gao, 2010. Chemical composition and size distributions of coastal aerosols observed on the US East Coast. *Mar. Chem.* 119, 77-90.  
doi: 10.1016/j.marchem.2010.01.002
- Yin J. and R.M. Harrison, 2008. Pragmatic mass closure study for PM<sub>10</sub>, PM<sub>2.5</sub> and PM<sub>10</sub> at roadside, urban background and rural sites. *Atmos. Environ.* 40, 980-988. doi: 10.1016/j.atmosenv.2007.10.005
- Yin J., R.M. Harrison, Q. Chen, A. Rutter and J.J. Scauer, 2010. Source apportionment of fine particles at urban background and rural sites in the UK atmosphere. *Atmos. Environ.* 44, 841-851.  
doi: 10.1016/j.atmosenv.2009.11.026